IEEE Access
Multidisciplinary ⋮ Rapid Review ⋮ Open Access Journal

Received 28 May 2024, accepted 12 July 2024, date of publication 17 July 2024, date of current version 26 July 2024.

Digital Object Identifier 10.1109/ACCESS.2024.3429551

THEORY

Robust Feedforward Control of Discrete Uncertain Systems Over a Finite Frequency Range

QINGFENG XIA[1,2], MENGHAN WEI[3], YIYANG CHEN[4], (Member, IEEE), LEI WANG[1], AND LIANGXIN DONG[3]

[1]School of Automation, Wuxi University, Wuxi 214105, China
[2]School of Management and Engineering, Nanjing University, Nanjing 210093, China
[3]School of Automation, Nanjing University of Information Science and Technology, Wuxi 214105, China
[4]School of Mechanical and Electrical Engineering, Soochow University, Suzhou 215137, China

Corresponding author: Qingfeng Xia (xqf@cwxu.edu.cn)

This work was supported in part by the 2022 China Higher Education Institution Industry-University-Research Innovation Fund—New Generation Information Technology Innovation Project under Grant 2022IT208, and in part by the Qing Lan Project of Jiangsu Province.

ABSTRACT In this paper, a novel robust iterative learning control strategy for linear discrete systems in a finite frequency domain is proposed. The strategy first converts the iterative learning control process into a discrete linear repeating system model by means of the equivalence transformation technique, and employs a convex bounded uncertainty domain to define the uncertainty range of the system. Subsequently, the control law design problem in discrete linear repetitive systems is solved by utilizing the generalized KYP lemma, which is transformed into the problem of solving linear matrix inequalities (LMIs). The designed control law is able to satisfy the robustness requirement in the direction of the iteration axis and ensure the monotonic convergence of the dynamic error between each experiment, so as to realize the expected control objective step by step. Finally, the advantages and practicality of the method are experimentally verified, and its potential limitations and constraints are analyzed and summarized.

INDEX TERMS Uncertainties, robust convergence, Kalman-Yakubovich-Popov, linear discrete system.

I. INTRODUCTION

Iterative learning control (hereinafter referred to as ''ILC'') is a control method for repetitive motions whose goal is to improve the tracking performance of a system by learning the behavior and applying repetitive strategies. The method works by continuously correcting the deviation between the actual and desired outputs of the system, rather than relying on an ideal control signal. Through many iterations, the output of the system will gradually approach the desired trajectory [1], [2], [3]. ILC technology offers a number of significant advantages, including its simplified controller design, low dependence on a priori knowledge, excellent adaptability, and simplified implementation in [4], [5], [6], and [7]. It has been applied to deal with many practical problems including industrial batch process [8], medical equipment [9], intelligent transportation system [10], flight control system [11]. In addition, ILC has been successfully applied in the field of vehicle trajectory tracking. ILC can adaptively adjust the control inputs based on previous tracking experience to cope with the influence of different road conditions, load changes or other environmental factors. Secondly, ILC can gradually accumulate experience and optimize the control strategy after performing trajectory tracking tasks for many times, so as to improve the tracking accuracy and robustness of the system. It can also learn and adjust online in a dynamic environment to cope with real-time changes in trajectory and environmental conditions, thus realizing more robust trajectory tracking performance [12].

According to the literature [13], ILC is defined in essence as a two-dimensional system model that unfolds its properties

The associate editor coordinating the review of this manuscript and approving it for publication was Laura Celentano.

along the time axis and the number of batches. In each iteration of the experiment, ILC system operates and learns processes along the timeline. At the end of experiment, the system is reset to its initial state, ready for the next experiment. By adopting a unified two-dimensional systems theoretical framework, the dynamic behavior of ILC system in the time dimension and its operational characteristics can be analyzed in depth, as well as the impact of change in the number of experiments on the performance of system. This analytical approach helps to fully understand the nature of learning process and effectively improve the transient response capability and tracking accuracy of system [14]. Furthermore, there are widespread uncertainties in practical industrial systems, such as measurement errors, external disturbances, sensor errors, etc, these uncertainties can lead to unstable dynamic performance of the system [15]. Therefore, studying the ILC problem of uncertain systems has important practical significance.

It is worth mentioning that two-dimensional system theory plays a key role in analyzing the dynamic performance and learning behavior of ILC. For discrete linear system with polyhedral uncertainties and actuator failures, a robust control law based on parameter dependent Lyapunov function is designed in [16]. Reference [17] transformed multi-stage batch processes into equivalent 2D switching fault-tolerant rosser models and designed a hybrid fault-tolerant law to ensure exponential operational stability. Based on the theoretical analysis of 2D roesser model, in the work of [18], it was explored the conditions for algorithm convergence in ILC and further proposed a new control strategy. The strategy effectively solves the point-to-point tracking problem by the method of trajectory update. Through an in-depth analysis of the state transfer matrix characteristics of the time-varying 2D model and the system response, a comprehensive predictive ILC algorithm is designed, aiming to improve the tracking accuracy and stability of the system.

However, the above ILC algorithm mainly relies on Lyapunov stability theory and may encounter difficulties in practical applications [19]. Especially when reference signals and operational specifications are involved, performance metrics and design specifications in the frequency domain are particularly critical. In addition, the above methods are more suitable for the study of nonlinear systems [20], whereas this paper focuses on the exploration of linear systems. Therefore, it becomes crucial to develop an adaptive ILC framework that can achieve the desired performance metrics in the specified frequency range. To meet specific specification requirements, this paper establishes a link between the frequency domain energy metrics and the conditions in the LMI format using the generalized KYP method. The generalized KYP method is chosen because it is not only widely applicable but also easy to solve, which makes the stability analysis and controller design for linear dynamic systems more convenient, efficient and reliable. The equivalence of this approach ensures that the redesigned ILC scheme can achieve the desired control performance in a predetermined frequency range. In addition, by introducing the theory of repetitive process stability, this study further deepens the understanding of ILC law in discrete linear dynamics models. The generalized KYP lemma has direct capability to address diverse performance specifications within finite frequency range in [21]. Reference [22] employs generalized KYP lemma to transform the analysis of system stability and control law design for discrete linear systems with polyhedral uncertainties and state delays. Following this lemma, the task can be reformulated in a finite frequency domain and the problem can be solved with the help of LMI. By introducing a state feedback mechanism, the system is able to remain stable and ensure robust stability even in the presence of intra-norm uncertainty. This mechanism not only enhances the robustness of system but also ensures the convergence of error in the monotonic test frequency direction in [23].

In the existing studies [24], [25], although the time lag and time variation in the system are considered, the exploration of the system uncertainty is neglected. Therefore, in this paper, we further explore robust ILC strategies for discrete linear systems with polyhedral uncertainty in a finite frequency domain based on previous studies. The research in this paper makes the following important contributions:

1) The article presents a comprehensive robust ILC strategy that is specifically designed for polyhedral uncertainty in discrete linear systems and modeled in the frequency domain.
2) For discrete linear repetitive operation modes in a specific frequency range, this paper constructs a new robust controller design scheme using the support of generalized KYP priming. The scheme not only satisfies the performance specification, but also ensures the stability of the system and monotonic convergence between experiments. In addition, this design methodology can be extended and applied to other control systems with similar characteristics, providing an effective design framework for these systems.
3) Through experimental verification, this paper confirms the feasibility of the proposed robust ILC strategy and controller design scheme, and provides solid support for its application in real systems.

In this article, symbols 0 and I denote the zero matrix and identity matrix, respectively, with suitable dimensions. For matrix Y, $Y > 0$ $(Y < 0)$, represents a positive definite (negative definite) matrix. $sym(Y)$ represents symmetric matrix $Y + Y^T$. $Y^{\perp}$ is orthogonal complement of matrix Y. Also, $diag\{Y_1, Y_2, \ldots, Y_n\}$ stands for diagonal matrix. The notation $*$ stands for transposition of elements in symmetric positions. Finally, $\rho(\cdot)$ represents spectral radius of matrix argument.

To proceed, following lemmas are widely used below.

Lemma 1 [26]: Let $\Gamma \in R^{p\times p}$ satisfy that $\Gamma = \Gamma^T$, Λ and Σ are matrices with columns p, there exists an invertible matrix W such that following matrix inequalities hold

$$\Gamma + sym\left\{\Lambda^T W \Sigma\right\} < 0 \tag{1}$$

only the following formula holds

$$\Lambda^{\perp T}\Gamma\Lambda^{\perp} < 0, \quad \Sigma^{\perp T}\Gamma\Sigma^{\perp} < 0 \tag{2}$$

Lemma 2 [27]: For a discrete linear time-invariant system represented by a transfer function matrix $G(z)$ and a frequency response matrix $G\left(e^{j\theta}\right) = C\left(e^{j\theta}I - A\right)^{-1}B + D$, the following conditions are equivalent.

i) Frequency domain inequality

$$\begin{bmatrix} G\left(e^{j\theta}\right) \\ I \end{bmatrix}^T \Pi \begin{bmatrix} G\left(e^{j\theta}\right) \\ I \end{bmatrix} < 0, \quad \forall\theta \in \Omega \tag{3}$$

where Π is a given real symmetric matrix, Ω denotes frequency range specified as in Table 1.

ii) There exist Hermitian matrices P and Q satisfying $Q > 0$ such that

$$\begin{bmatrix} A & B \\ I & 0 \end{bmatrix}^T (\Phi \otimes P + \Psi \otimes Q) \begin{bmatrix} A & B \\ I & 0 \end{bmatrix} + \Theta < 0 \tag{4}$$

where

$$\Phi = \begin{bmatrix} -1 & 0 \\ * & 1 \end{bmatrix}, \quad \Psi = \begin{bmatrix} \tau & v \\ * & \varsigma \end{bmatrix}. \tag{5}$$

Table 1 shows the values of τ, υ, and ς under different conditions of $\theta \in \Omega$.

TABLE 1. System frequency range.

Symbol	Low frequency	Middle frequency	High frequency
Ω	$\theta \leq \theta_l$	$\theta_1 \leq \theta \leq \theta_2$	$\theta \geq \theta_h$
τ	0	0	0
υ	1	$e^{j(\theta_1+\theta_2)/2}$	-1
ς	$-2\cos(\theta_l)$	$-2\cos((\theta_1-\theta_2)/2)$	$2\cos(\theta_h)$

II. PROBLEMS DESCRIPTION

Consider discrete linear repetitive processes within finite time intervals, whose state space model is represented as

$$\begin{cases} x_k(n+1) = Ax_k(n) + Bu_k(n) \\ y_k(n) = Cx_k(n), 0 \leq n \leq \alpha - 1 \end{cases} \tag{6}$$

where $k \geq 0$ stands for the number of iterations, and $\alpha < \infty$ is period length. In addition, $x_k(n) \in R^n$, $u_k(n) \in R^m$ and $y_k(n) \in R^l$ represent state vector, control input and output of system at the k-th n time, respectively. It is generally believed that at the beginning of each experiment, $x_k(0) = x_0$ is defined, and the entry in the initial experimental output vector $y_0(p)$ is a known function of entire experimental length with respect to P. Furthermore, if the matrices in system (6) are uncertain, it is assumed that they depend on the given expression for real parameter vector ξ in the polyhedron set as

$$A = \sum_{i=1}^{M} \xi_i A_i, B = \sum_{i=1}^{M} \xi_i B_i, C = \sum_{i=1}^{M} \xi_i C_i \tag{7}$$

where A_i, B_i and C_i define vertices of polyhedron, and M represents the number. The value of term i in Eq.(7) should be in the range of 1 to M to correspond to the description of each vertex and uncertainty range of polyhedron. The convex bounded uncertainty domain is defined as Ω_0 in which the uncertain model matrix is included

$$\Omega_0 = \{(A, B, C)|(A, B, C) = \sum_{i=1}^{M} \xi_i(A_i, B_i, C_i)\} \tag{8}$$

where $\xi_i \geq 0$, $\sum_{i=1}^{M} \xi_i = 1$.

Introduce reference trajectory $y_d(n)$ while defining tracking error of experiment k

$$e_k(n) = y_d(n) - y_k(n). \tag{9}$$

ILC control rate of system (6) is determined by the combination of previous experimental input and correction terms within ILC strategy for current experimental input

$$\begin{cases} u_{k+1}(n) = u_k(n) + \Delta u_{k+1}(n) \\ u_0(n) = 0, n \in [0, \alpha - 1] \end{cases} \tag{10}$$

where $u_0(n)$ denotes initial input vector of experiment, $\Delta u_k(n)$ is called a correction calculated using previous experimental information. And analyze it by introducing the intermediate vector $\eta_{k+1}(n+1)$

$$\eta_{k+1}(n+1) = x_{k+1}(n) - x_k(n). \tag{11}$$

In addition, with the progress of experiment, the convergence speed of output trajectory of control system is improved through learning experience. Integration of experimental tracking errors can serve as an extended experience to improve control performance. Error compensator learns from PD-type ILC controller to generate a feedforward PD-type ILC. As research in literature [25], [28], state feedback controllers are applications for enhancing system robust stability, using PD-type learning terms for experimental error convergence, and introducing tracking error compensators to improve tracking performance during the experimental process. Its dynamic model is

$$\hat{x}_k(n+1) = A_e\hat{x}_k(n) + B_e e_k(n+1) \tag{12}$$

where $\hat{x}_k(n) \in R^n$ represents state vector of compensator, $\{A_e, B_e\}$ represents compensator structure matrix, with appropriate dimensions and values. According to it, compensator structure in Eq. (12) can be determined. Reference [25] discusses design process of error compensator and provides guidance for design method of compensator parameters. PID-type selection error compensator is used in this paper, where

$$A_e = \begin{bmatrix} 0 & 0 & 0 \\ 0 & I & 0 \\ -I & 0 & 0 \end{bmatrix}, \quad B_e = \begin{bmatrix} I \\ I \\ I \end{bmatrix},$$

$$\hat{x}_k(n) = \begin{bmatrix} e_k(n) \\ \sum_{i=1}^{n} e_k(i) \\ e_k(n) - e_k(n-1) \end{bmatrix}. \tag{13}$$

III. ILC DESIGN IN REPETITIVE PROCESS FORM

The design of ILC process in this paper utilize the theory of repeated process stability. To enhance the tracking ability of system and fully leverage ILC law. Update law of formula (10) is in the following form

$$\Delta u_{k+1}(n) = K_1\eta_{k+1}(n+1) + K_2\hat{x}_{k+1}(n) + K_3 e_k(n) + K_4(e_k(n+1) - e_k(n)) \tag{14}$$

where K_1 represents the state feedback controller parameter, K_2 denotes the gain matrix of the error compensation controller, K_3 and K_4 are the roburst ILC learning gains of previous trial tracking error $e_k(n)$. When $K_2 = 0$, it is the control law of PD-type ILC.

By applying the Eq. (6) to Eq.(12), this paper derives the resultant system model

$$\begin{cases} \eta_{k+1}(n+1) = A\eta_{k+1}(n) + B\Delta u_{k+1}(n) \\ \hat{x}_k(n+2) = A_e\hat{x}_k(n+1) - B_eCA\eta_{n+1}(n) \\ \qquad -B_e e_{n-1}(n+1) - B_eCB\Delta u_{n+1}(n) \\ e_k(n+1) = e_{k-1}(n+1) - CA\eta_{n+1}(n) - CB\Delta u_{k+1}(n) \end{cases} \tag{15}$$

To simplify the calculation, setting $L = K_3 - K_4$. Meanwhile, the augmented state vector is defined as

$$X_k(n) = [\eta_{k+1}(n)^T \, \hat{x}_k(n+1)^T \, e_{k-1}(n+1)^T]^T \tag{16}$$

and application of (14) to (15), turning it into

$$\begin{cases} X_k(n+1) = A_1X_k(n) + B_1e_{k-1}(n+1) \\ e_k(n+1) = C_1X_k(n) + D_1e_{k-1}(n) \end{cases} \tag{17}$$

where

$$A_1 = \hat{A}_1 + \hat{B}_1\hat{K}, \quad B_1 = \hat{B}_2 + \hat{B}_1K_4,$$
$$C_1 = \hat{C}_1(\hat{A}_1 + \hat{B}_1\hat{K}), \quad D_1 = I - CBK_4$$
$$\hat{A}_1 = \begin{bmatrix} A & 0 & 0 \\ -B_eCA & A_e & 0 \\ 0 & 0 & 0 \end{bmatrix}, \quad \hat{B}_1 = \begin{bmatrix} B \\ -B_eCB \\ 0 \end{bmatrix},$$
$$\hat{B}_2 = \begin{bmatrix} 0 \\ B_e \\ I \end{bmatrix}, \quad \hat{K} = \begin{bmatrix} K_1 & K_2 & L \end{bmatrix},$$
$$\hat{C}_1 = \begin{bmatrix} -C & 0 & 0 \end{bmatrix}.$$

In addition, the model (17) is called the tracking error transfer function matrix, which associates previous test error with current test error

$$\Delta u_{k+1}(n) = K_1\eta_{k+1}(n+1) + K_2\hat{x}_{k+1}(n) + K_3e_k(n) + K_4(e_k(n+1) - e_k(n)). \tag{18}$$

Finally, the robust stability and controller design issues of the ILC system described in model (17) are studied in the frequency domain.

IV. STABILITY CONDITIONS WITHIN A FINITE FREQUENCY RANGE

The following lemma describes the conditions that need to be met for the stability of the ILC dynamic model described in model (17) along the number of experiments.

Lemma 3 [29]: Assuming that coefficients $\{A_1, B_1\}$ are controllable and coefficients $\{C_1, A_1\}$ are observable, the stability of linear repetitive process described by equation (17) is determined by the validity of following inequalities:

i) $\rho(D_1) < 1$;
ii) $\rho(A_1) < 1$;
iii) The transfer function $G(z) = C_1(zI - A_1)^{-1}B_1 + D_1$ has all eigenvalue magnitudes strictly less than 1 on the unit circle $|z| = 1$.

Each condition in lemma has a specific physical meaning. Condition (i) guarantees the asymptotic stability of experiment, and condition (ii) ensures convergence over the repetition period time. It can be intuitively expected that this condition represents the robust stability of the current experimental state dynamics. For condition (iii), it is necessary to calculate the modulus of all eigenvalues on the unit circle, which makes calculation difficult. In addition, the limited frequency range of the proposed control system work performance has important practical significance, especially in ILC systems where the main frequency distribution of the reference signal is within the limited range. Therefore, monotone convergent ILC algorithm is designed by means of generalized KYP lemma in a specific frequency range. The basic inequality obtained by applying condition (iii) of lemma 1 is

$$\rho(G(e^{j\theta})) < 1, \forall\theta \in \Omega \tag{19}$$

and Ω denotes the finite frequency ranges defined in Table1. Alternatively, a Hermitian matrix $H(e^{j\theta}) > 0$ can be used to represent the final result, such that

$$\begin{bmatrix} G(e^{j\theta}) \\ I \end{bmatrix}^T \begin{bmatrix} H(e^{j\theta}) & 0 \\ 0 & -H(e^{j\theta}) \end{bmatrix} \begin{bmatrix} G(e^{j\theta}) \\ I \end{bmatrix} < 0. \tag{20}$$

Solving Eq. (20) poses a challenge due to the interdependency of $H\left(e^{j\theta}\right)$ and θ. Therefore, a multiplier such as $H\left(e^{j\theta}\right) = H$ or $H\left(e^{j\theta}\right) = I$ can be applied, giving up its conservatism to simplify the calculation. Next, set the matrix Π in Eq. (3) as

$$\Pi = \begin{bmatrix} H & 0 \\ 0 & -H \end{bmatrix}, H > 0. \tag{21}$$

The new number along the test error based on LMI monotone convergence condition and the ILC design limited frequency-domain performance can be determined by the following result.

Lemma 4 [18]: If positive definite matrices S, P, Q, R, and matrices W_1, W_2 are existent, following inequality holds

$$A_1^TSA_1 - S < 0 \tag{22}$$

then, within the limited frequency range defined in Table 1, system (17) under ILC is stable and actual output of the control system asymptotically tracks the desired trajectory.

$$\begin{bmatrix} -P+\tau Q & \upsilon Q - W_1 & 0 \\ * & P+\varsigma Q + sym(A_1^T W_1) + C_1^T R C_1 & W_1^T B_1 + C_1^T R D_1 \\ * & * & -R + D_1^T R D_1 \end{bmatrix} < 0 \tag{23}$$

In this paper, we focus on the uncertainty of the output matrix C in Theorem 1 in finite frequency domain range, remove the constraints on C, and discuss and prove it exhaustively. In dealing with uncertainty, the ILC designed in this paper not only considers the uncertainty of system dynamics, but also includes the uncertainty of the observation equations. This is different from the traditional PD-type ILC, which usually does not involve the variability of the output matrix C, as it mainly focuses on the iterative learning process in the controller design. In addition, Eq. (24) is introduced to relate the matrix variables to the affine parameters of matrix separation of the discrete linear system. This move implies that when dealing with the case described by the polyhedral Eq. (8), one is not only concerned with the linear nature of the system, but must also take into account the uncertainties inherent in the model.

$$\begin{aligned} \hat{P}(\xi) &= \sum_i^N \xi_i \hat{P}_i, \qquad \hat{P}_i > 0, \quad i = 1, \ldots, N. \\ \hat{Q}(\xi) &= \sum_i^N \xi_i \hat{Q}_i, \qquad \hat{Q}_i > 0, \quad i = 1, \ldots, N. \\ \hat{R}(\xi) &= \sum_i^N \xi_i \hat{R}_i, \qquad \hat{R}_i > 0, \quad i = 1, \ldots, N. \\ \hat{S}(\xi) &= \sum_i^N \xi_i \hat{S}_i, \qquad \hat{S}_i > 0, \quad i = 1, \ldots, N. \end{aligned} \tag{24}$$

Theorem 1: ILC learning law (10) and its correction term (14) are applied to a discrete linear system represented by (6). (7) and (8) define system uncertainty. If matrices $\hat{S}_i > 0$, $\hat{P}_i > 0$, $\hat{R}_i > 0$, $\hat{W}_1$, $\hat{W}_2$, Y_1 and Y_2 exist, make the following inequality hold for $1 \le i \le j \le N$

$$Z_{ii} < 0 \tag{25}$$
$$Z_{ij} + Z_{ji} < 0 \tag{26}$$
$$M_{ii} < 0 \tag{27}$$
$$M_{ij} + M_{ji} < 0 \tag{28}$$

where

$$Z_{ii} = \begin{bmatrix} -\hat{S}_i & \hat{A}_{1ii}\hat{W}_1 + \hat{B}_{1ii}Y_1 \\ * & \hat{S}_i - \hat{W}_1 - \hat{W}_1^T \end{bmatrix},$$

$$Z_{ij} = \begin{bmatrix} -\hat{S}_i & \hat{A}_{1ij}\hat{W}_1 + \hat{B}_{1ij}Y_1 \\ * & \hat{S}_i - \hat{W}_1 - \hat{W}_1^T \end{bmatrix},$$

$$M_{ii} = \begin{bmatrix} -\hat{P}_i + \tau\hat{Q}_i & \upsilon\hat{Q}_i - \hat{W}_1 & 0 & 0 \\ * & \hat{P}_i + \varsigma\hat{Q}_i + sym(\hat{A}_{1ii}\hat{W}_1 + \hat{B}_{1ii}Y_1) & \hat{B}_2 + B_{1ii}Y_2 & (\hat{C}_{1i}\hat{A}_{1ii}\hat{W}_1 + \hat{C}_{1i}\hat{B}_{1ii}Y_1)^T \\ * & * & -\hat{R}_i & (\hat{W}_2 - C_iB_iY_2)^T \\ * & * & * & \hat{R}_i - \hat{W}_2 - \hat{W}_2^T \end{bmatrix},$$

$$M_{ij} = \begin{bmatrix} -\hat{P}_j + \tau\hat{Q}_j & \upsilon\hat{Q}_j - \hat{W}_1 & 0 & 0 \\ * & \hat{P}_j + \varsigma\hat{Q}_j + sym(\hat{A}_{1ij}\hat{W}_1 + \hat{B}_{1ij}Y_1) & \hat{B}_2 + B_{1ij}Y_2 & (\hat{C}_{1i}\hat{A}_{1ij}\hat{W}_1 + \hat{C}_{1i}\hat{B}_{1ij}Y_1)^T \\ * & * & -\hat{R}_j & (\hat{W}_2 - C_iB_jY_2)^T \\ * & * & * & \hat{R}_i - \hat{W}_2 - \hat{W}_2^T \end{bmatrix},$$

$$\hat{A}_{1ii} = \begin{bmatrix} A_i & 0 & 0 \\ -B_eC_iA_i & A_e & 0 \\ 0 & 0 & 0 \end{bmatrix}, \quad \hat{B}_{1ii} = \begin{bmatrix} B_i \\ -B_eC_iA_i \\ 0 \end{bmatrix},$$

$$\hat{A}_{1ij} = \begin{bmatrix} A_j & 0 & 0 \\ -B_eC_iA_j & A_e & 0 \\ 0 & 0 & 0 \end{bmatrix}, \quad \hat{B}_{1ii} = \begin{bmatrix} B_j \\ -B_eC_iA_j \\ 0 \end{bmatrix}.$$

Then, within the limited frequency range defined in Table 1, system (17) under ILC is stable and actual output of the control system asymptotically tracks desired trajectory.

Proof 1: It is shown by Lemma 4 that W_1, W_2 are non-singular matrices and are invertible, while it can be obtained that $S_i > 0$, set $\hat{W}_1 = W_1^{-1}$, $\hat{W}_2 = W_2^{-1}$, $\hat{S}_i = \hat{W}_1 S_i \hat{W}_1^T$ and Eq. (22) can be rewritten as

$$\begin{bmatrix} S_i - W_1 - W_1^T & W_1\hat{A}_i \\ * & -S_i \end{bmatrix} < 0. \tag{29}$$

Multiplying Eq. (29) by $diag\{\ \hat{W}_1^T \ \ \hat{W}_1^T\ \}$ and its transpose before and after, respectively, we get

$$\begin{bmatrix} \hat{S}_i - \hat{W}_1 - \hat{W}_1^T & \left(\hat{A}_{1ii}\hat{W}_1 + \hat{B}_{1ii}Y_1\right) \\ * & -\hat{S}_i \end{bmatrix} < 0. \tag{30}$$

Eq. (30) is equivalent to $Z_{ii} < 0$ in the theorem, so (25) is proved. The same reasoning proves that $Z_{ij} < 0$.

Next, left and right multiplying the inequality (27) by $diag\left\{\hat{W}_1^{-1},\ \hat{W}_1^{-1},\ \hat{W}_2^{-1},\ \hat{W}_2^{-1}\right\}$ and its transpose, respectively, and introducing the following change of variables

$$\begin{aligned} &W_1 = \hat{W}_1^{-1}, W_2 = \hat{W}_2^{-1}, \quad S_i = \hat{W}_1^{-T}\hat{S}_i\hat{W}_1^{-1} \\ &P_i = \hat{W}_1^{-T}\hat{P}_i\hat{W}_1^{-1}, \quad Q_i = \hat{W}_1^{-T}\hat{Q}_i\hat{W}_1^{-1}, \\ &R_i = \hat{W}_2^{-T}\hat{R}_i\hat{W}_2^{-1}, \end{aligned}$$

gives

$$\begin{bmatrix} -P_i + \tau Q_i & \upsilon Q_i - W & 0 & 0 \\ * & P_i + \varsigma Q_i + sym\left(A_{1ii}W_1 + B_{1ii}Y_1\right) & B_2 + B_{1ii}Y_2 & (C_{1i}A_{1ii}W_1 + C_{1i}B_{1ii}Y_1)^T \\ * & * & -R_i & (W_2 - C_iB_iY_2) \\ * & * & * & R_i - W_2 - W_2^T \end{bmatrix} < 0. \tag{31}$$

The above inequality can be equivalently rewritten as

$$\Gamma_2 + sym\left\{\Lambda_2^T M \Sigma_2\right\} < 0. \tag{32}$$

where

$$\Gamma_2 = \begin{bmatrix} -P_i + \tau Q_i & \upsilon Q_i - W_1 & 0 & 0 \\ * & P_i + \varsigma Q_i + sym\left(A_{1ii}W_1 + B_{1ii}Y_1\right) & B_2 + B_{1ii}Y_2 & 0 \\ * & * & -R_i & 0 \\ * & * & * & -R_i \end{bmatrix}$$

$$\Lambda_2 = \begin{bmatrix} 0 & (C_{1i}A_{1ii}W_1 + C_{1i}B_{1ii}Y_1)^T & (W_2 - C_iB_iY_2) & -W_2 \end{bmatrix}$$
$$M = I, \Sigma_2 = \begin{bmatrix} 0 & 0 & 0 & I \end{bmatrix}$$

and W_2 is a slack matrix variable. Also, the matrices $\Lambda_2^{\perp}$ and $\Sigma_2^{\perp}$, whose columns form a basis for the null spaces of Λ_2 and Σ_2, are respectively given by

$$\Lambda_2^{\perp} = \begin{bmatrix} I & 0 & 0 \\ 0 & W_2 & 0 \\ 0 & 0 & W_2 \\ 0 & (C_{1i}A_{1ii}W_1 + C_{1i}B_{1ii}Y_1)^T & (W_2 - C_iB_iY_2) \end{bmatrix}$$
$$\Sigma_2^{\perp} = \begin{bmatrix} I & 0 & 0 \\ 0 & I & 0 \\ 0 & 0 & I \\ 0 & 0 & 0 \end{bmatrix}$$

Employing lemma 2 yields

$$\left(\Lambda_2^{\perp}\right)^T \Gamma_2 \Lambda_2^{\perp} < 0 \tag{33}$$
$$\left(\Sigma_2^{\perp}\right)^T \Gamma_2 \Sigma_2^{\perp} < 0 \tag{34}$$

Lemma 1 is satisfied, so Eq. (27) holds. Similarly, $M_{ij} < 0$ holds.

We know that for $i = 1, \cdots, N$ holds for all LMIs (25), (27). These LMIs are then multiplied by the uncertainty parameter and the sum of LMIs (25)-(26) and LMIs (27)-(28), respectively, yields

$$\sum_{i=1}^{N} \xi_i Z_{ii} + \sum_{i=1}^{N}\sum_{i<j}^{N} \xi_i\xi_j(Z_{ij} + Z_{ji}) < 0 \tag{35}$$
$$\sum_{i=1}^{N} \xi_i M_{ii} + \sum_{i=1}^{N}\sum_{i<j}^{N} \xi_i\xi_j(M_{ij} + M_{ji}) < 0 \tag{36}$$

Clearly, the above inequality can be rewritten as

$$Z(\xi) < 0, M(\xi) < 0. \tag{37}$$

Among them, the affine parameter correlation matrices of Eqs. (7) and (24) were used. So the application of lemma 4 means that inequalities (25) to (28) are feasible for all $i = 1, \cdots, N$ and the proof is complete.

It is assumed the output matrix C is fixed, i.e., $C_i = C$, for all $i = 1, \cdots, N$, the LMI-base conditions of (25)-(28) reduces to

$$Z_{ii} < 0 \tag{38}$$
$$M_{ii} < 0. \tag{39}$$

The ILC update law matrix is

$$\begin{bmatrix} K_1 & K_2 & L \end{bmatrix} = Y_1\hat{W}_1^{-1}, \quad K_4 = Y_2\hat{W}_2^{-1}, \; K_3 = L + K_4.$$

V. EXPERIMENTAL VALIDATION

The experimental machining platform shown in Fig. 1 is an integral XY system with crossed roller bearings and is a two-dimensional displacement device. The crossed roller bearings are specially designed to carry both radial and axial forces with an accuracy of 3 microns in each axis, and have excellent rigidity and repeatability to provide stable and precise motion. Therefore, the x-axis can be utilized for precise positioning and movement for high precision tracking.

To verify performance of ILC design scheme mentioned in this article, experimental verification is conducted on the design case provided in this section. Consider the uncertain linear system as shown in Eq. (7), and its parameter matrix is given by the following matrices

$$A(\xi) = \xi_1 \begin{bmatrix} 1 & 1.383 \\ 0.15 & 1.082 \end{bmatrix} + \xi_2 \begin{bmatrix} 1 & 1.021 \\ 0.30 & 0.920 \end{bmatrix},$$
$$B(\xi) = \xi_1 \begin{bmatrix} 0.512 \\ 0.207 \end{bmatrix} + \xi_2 \begin{bmatrix} 0.476 \\ 0.352 \end{bmatrix},$$
$$C(\xi) = \xi_1 \begin{bmatrix} 0.46 & 0.02 \end{bmatrix} + \xi_2 \begin{bmatrix} 0.55 & 0.10 \end{bmatrix} \tag{40}$$

where ξ_1, ξ_2 are uncertainty parameters varying from $[0, 1]$, satisfy $\xi_1 + \xi_2 = 1$. The effective harmonics of the reference trajectory yd(t) in Fig. 2 are varied between 0 and 10 Hz, which belongs to the low frequency range. Therefore, $\theta_l = 0.3142$, $\tau = 0$, $\upsilon = 1$, $\varsigma = -2\cos(\theta_l)$.

Robust feedforward ILC gain matrix is as follows

$$K_1 = \begin{bmatrix} -3.4544 & 0.8633 \end{bmatrix},$$
$$K_2 = \begin{bmatrix} -0.2467 & 4.4198 & -0.2425 \end{bmatrix},$$
$$K_3 = 3.9086, \quad K_4 = 3.9964. \tag{41}$$

The system is modeled and experimented based on the above values. The output trajectory of the model at different number of iterations is shown in Fig. 2. It can be clearly seen from the figure that there is a large discrepancy between the system output and the desired trajectory at the first iteration. However, through continuous learning and adjustment, the system gradually approaches the desired trajectory in each subsequent iteration, and finally realizes the accurate tracking of the desired trajectory. These experimental results fully demonstrate the effectiveness and accuracy of the algorithm.

To investigate the advantages of robust feed-forward ILC, its performance is compared with PD-type ILC. The controller form of PD-type ILC is

$$\Delta u_{k+1}(n) = K_1\eta_{k+1}(n+1) + K_3e_k(n) + K_4(e_k(n+1) - e_k(n)) \tag{42}$$

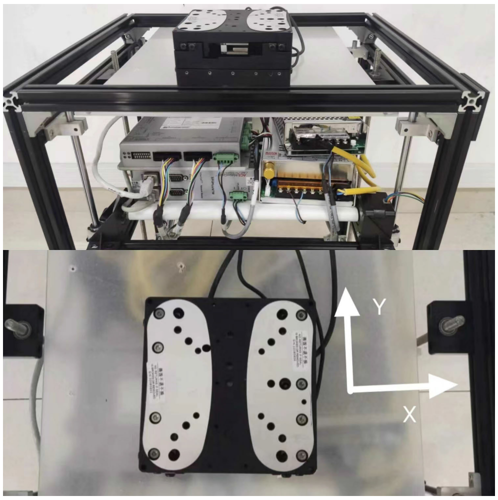

FIGURE 1. Monolithic XY platform. Dimensions are 125 mm long, 125 mm wide and 60 mm high.

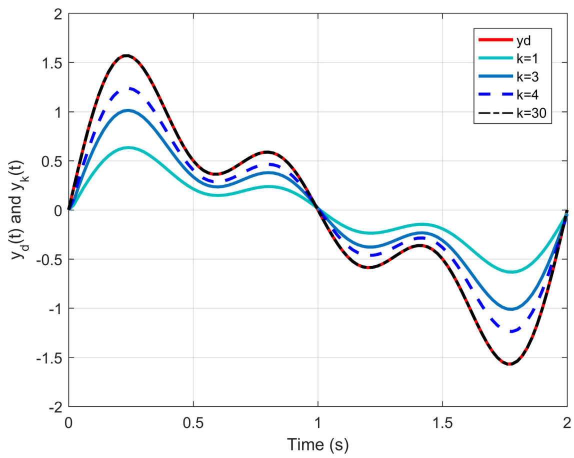

FIGURE 2. Output trajectories from execution of Algorithm 1 in iterative trials.

and the corresponding controller matrices are given as

$$K_1 = \begin{bmatrix} -2.6159 & -1.4627 \end{bmatrix},$$
$$K_3 = 2.9064, \quad K_4 = 2.6810.$$

To explore the tracking effect of different frequency domain ranges in the low frequency range, the spectrograms of the reference trajectories of the two algorithms are designed as shown in Fig. 3. Here the system iteration duration is set to be $1s$ and sampling frequency to 100 Hz.

The Root Mean Square (RMS) is introduced to measure the error size of the two algorithms, which is calculated as follows

$$RMS(e_k) = \sqrt{\frac{1}{H}\sum\nolimits_{n=1}^{H} e_k^2(n)}. \tag{43}$$

By comparing the RMS values of the two experiments in Fig. 4, it is clearly observed that the proposed method

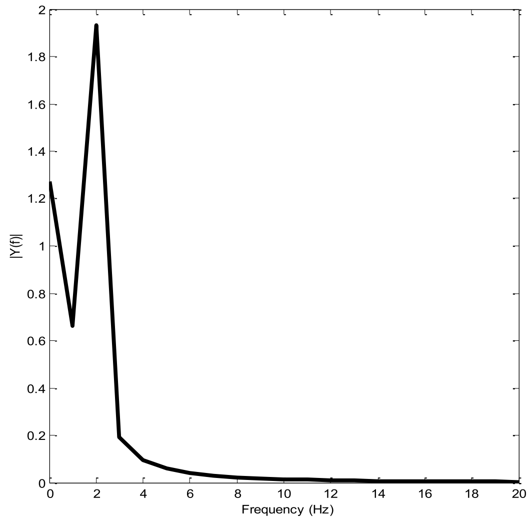

FIGURE 3. The corresponding frequency spectrum.

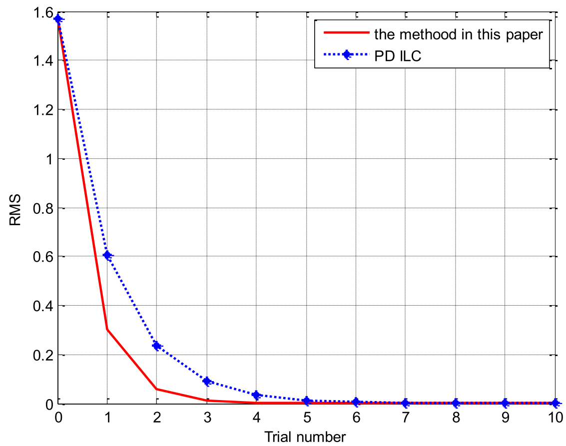

FIGURE 4. Comparison of the RMS of two algorithms.

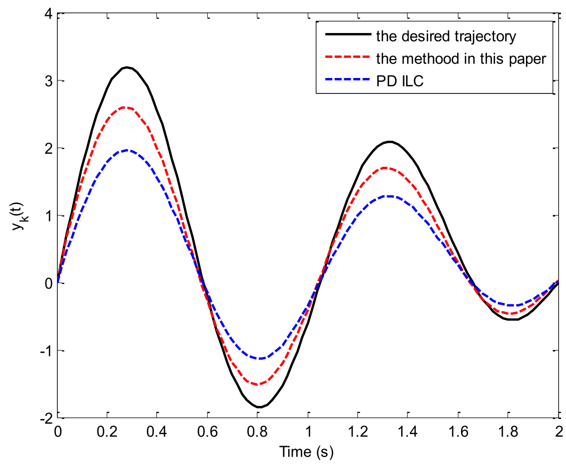

FIGURE 5. Output trajectories of both algorithms under the 1st iteration cycle.

in this paper converges faster. Fig. 5 shows the tracking accuracy of the output trajectories of the proposed algorithm and the PD-type algorithm at the 1st iteration. Fig. 6, Fig. 7,

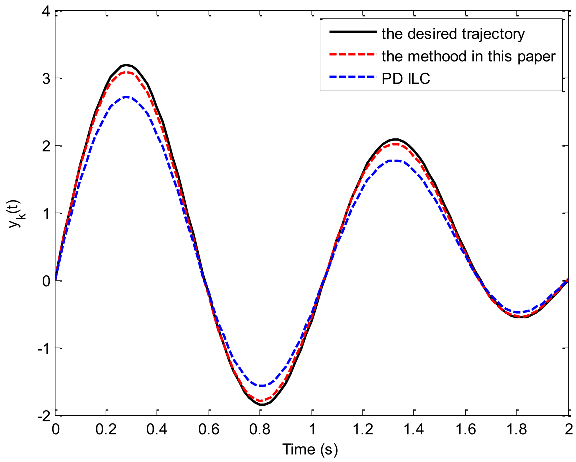

FIGURE 6. Output trajectories of both algorithms under the 2nd iteration cycle.

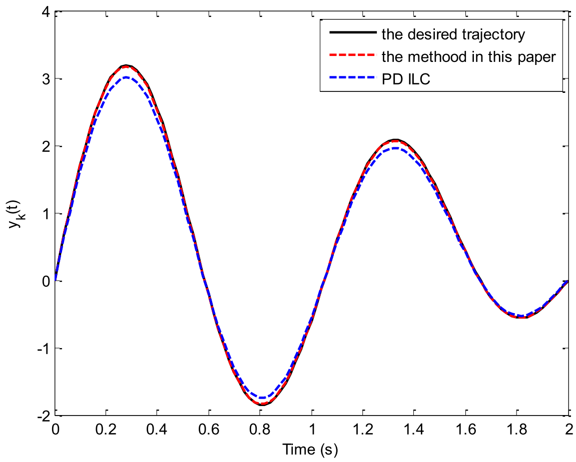

FIGURE 7. Output trajectories of both algorithms under the 3rd iteration cycle.

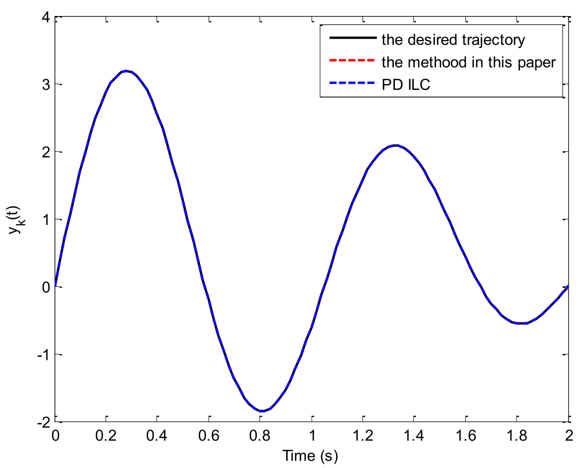

FIGURE 8. Output trajectories of both algorithms under the 10th iteration cycle.

and Fig. 8 show the tracking accuracy of the two algorithms at the 2nd, 3rd, and 10th iterations, respectively. The black solid line is the desired trajectory, the red solid line is the method designed in this paper, and the blue dashed line is the PD-type ILC. It is observed from Fig. 5 to Fig. 8 that both ILCs can provide robust stability and monotonic error convergence as experiment progresses. In addition, the convergence error rate of the algorithm proposed in this paper is improved compared to the PD-type ILC algorithm, which allows for more accurate tracking of the reference trajectory. This further validates the performance advantages of the robust feedforward ILC algorithm.

VI. CONCLUSION AND FUTURE WORK

For discrete linear systems with polyhedral uncertainty, the robust feedforward ILC strategy is studied in detail in this article. In frequency domain, a controller with good robustness and adaptability is designed by conducting several tests on the controlled object and analyzing the stability of system by using the statistical property of repeated process. Then, generalized KYP lemma is used to derive the constraints of controller parameters, which ensures that system has good tracking accuracy and stability in practical applications. Finally, results provide evidence of the effectiveness and practicality of the proposed scheme for the specified class of linear discrete systems with polytopic uncertainties.

However, in practice, obtaining the system matrix described in (8) is difficult and the potential actuator variance is not considered in this paper. Therefore, uncertainty identification should be one of our future tasks, and by identifying and modeling the uncertainty of the system, we can better adapt to the changes and uncertainties in the real environment, so as to improve the feasibility of the algorithms and extend their applications in various application scenarios. In addition, the effects of different types of disturbances on the stability and performance of the control system will be explored. The algorithm will be further optimized through the combination of theory and experiment.

REFERENCES

[1] D. Shen, "Iterative learning control with incomplete information: A survey," *IEEE/CAA J. Autom. Sinica*, vol. 5, no. 5, pp. 885–901, Sep. 2018.

[2] Y. Liu, X. Ruan, and X. Li, "Optimized iterative learning control for linear discrete-time-invariant systems," *IEEE Access*, vol. 7, pp. 75378–75388, 2019.

[3] Y. Chen and C. T. Freeman, "Iterative learning control for piecewise arc path tracking with validation on a gantry robot manufacturing platform," *ISA Trans.*, vol. 139, pp. 650–659, Aug. 2023.

[4] H. Tao, J. Li, Y. Chen, V. Stojanovic, and H. Yang, "Robust point-to-point iterative learning control with trial-varying initial conditions," *IET Control Theory Appl.*, vol. 14, no. 19, pp. 3344–3350, Dec. 2020.

[5] Y. Chen, B. Chu, and C. T. Freeman, "Iterative learning control for path-following tasks with performance optimization," *IEEE Trans. Control Syst. Technol.*, vol. 30, no. 1, pp. 234–246, Jan. 2022.

[6] S. Guan, Z. Zhuang, H. Tao, Y. Chen, V. Stojanovic, and W. Paszke, "Feedback-aided PD-type iterative learning control for time-varying systems with non-uniform trial lengths," *Trans. Inst. Meas. Control*, vol. 45, no. 11, pp. 2015–2026, Jul. 2023.

[7] M. Pierallini, F. Angelini, R. Mengacci, A. Palleschi, A. Bicchi, and M. Garabini, "A robust iterative learning control for continuous-time nonlinear systems with disturbances," *IEEE Access*, vol. 9, pp. 147471–147480, 2021.

[8] Y. Chen, W. Jiang, and T. Charalambous, "Machine learning based iterative learning control for non-repetitive time-varying systems," *Int. J. Robust Nonlinear Control*, vol. 33, no. 7, pp. 4098–4116, May 2023.

[9] Y. Huo, Q. Tao, and J. Hu, "Cooperative control for multi-intersection traffic signal based on deep reinforcement learning and imitation learning," *IEEE Access*, vol. 8, pp. 199573–199585, 2020.

[10] Y. Chen, B. Chu, and C. T. Freeman, "Iterative learning control for robotic path following with trial-varying motion profiles," *IEEE/ASME Trans. Mechatronics*, vol. 27, no. 6, pp. 4697–4706, Dec. 2022.

[11] J. P. Emelianova, "Iterative learning control for a discrete-time system with changing reference trajectory under uncertainty," *Autom. Remote Control*, vol. 83, no. 9, pp. 1452–1466, Sep. 2022.

[12] S. Kuutti, R. Bowden, Y. Jin, P. Barber, and S. Fallah, "A survey of deep learning applications to autonomous vehicle control," *IEEE Trans. Intell. Transp. Syst.*, vol. 22, no. 2, pp. 712–733, Feb. 2021.

[13] R. M. Asl and A. Madady, "Stabilization of two-dimensional mixed continuous-discrete-time systems via dynamic output feedback with application to iterative learning control design," *Trans. Inst. Meas. Control*, vol. 44, no. 1, pp. 172–187, Jan. 2022.

[14] K. Wan and H. Xie, "Frequency-domain based iterative learning control for 2-D discrete systems," *IEEE Access*, vol. 11, pp. 62180–62186, 2023.

[15] C. H. Dinh, V. T. Mai, and T. H. Duong, "New results on stability and stabilization of delayed caputo fractional order systems with convex polytopic uncertainties," *J. Syst. Sci. Complex.*, vol. 33, no. 3, pp. 563–583, Jun. 2020.

[16] O. Khan, G. Mustafa, A. Q. Khan, M. Abid, and M. Ali, "Fault-tolerant robust model-predictive control of uncertain time-delay systems subject to disturbances," *IEEE Trans. Ind. Electron.*, vol. 68, no. 11, pp. 11400–11408, Nov. 2021.

[17] L. Wang, F. Liu, J. Yu, P. Li, R. Zhang, and F. Gao, "Iterative learning fault-tolerant control for injection molding processes against actuator faults," *J. Process Control*, vol. 59, pp. 59–72, Nov. 2017.

[18] W. Zou, Y. Shen, W. Paszke, and H. Tao, "Robust feedback feed-forward PD-type iterative learning control for uncertain discrete systems over finite frequency ranges," *Trans. Inst. Meas. Control*, vol. 44, no. 14, pp. 2850–2862, Oct. 2022.

[19] F. Memon and C. Shao, "Data-driven optimal PID type ILC for a class of nonlinear batch process," *Int. J. Syst. Sci.*, vol. 52, no. 2, pp. 263–276, Jan. 2021.

[20] L. Wang, Z. Huangfu, R. Li, X. Wen, Y. Sun, and Y. Chen, "Iterative learning control with parameter estimation for non-repetitive time-varying systems," *J. Franklin Inst.*, vol. 361, no. 3, pp. 1455–1466, Feb. 2024.

[21] W. Paszke, E. Rogers, and K. Gałkowski, "Experimentally verified generalized KYP lemma based iterative learning control design," *Control Eng. Pract.*, vol. 53, pp. 57–67, Aug. 2016.

[22] Y. Wei and X. Li, "Robust iterative learning control for linear continuous systems with vector relative degree under varying input trail lengths and random initial state shifts," *Int. J. Robust Nonlinear Control*, vol. 31, no. 2, pp. 609–622, Jan. 2021.

[23] D. Meng and J. Zhang, "Convergence analysis of robust iterative learning control against nonrepetitive uncertainties: System equivalence transformation," *IEEE Trans. Neural Netw. Learn. Syst.*, vol. 32, no. 9, pp. 3867–3879, Sep. 2021.

[24] R. Maniarski, W. Paszke, E. Rogers, and H. Tao, "Repetitive process based design of PD-type iterative learning control laws for batch processes with time-delays," *IFAC-PapersOnLine*, vol. 56, no. 2, pp. 1901–1906, 2023.

[25] X. Li and X. Hou, "Robust design of iterative learning control for a batch process described by 2D Roesser system with packet dropouts and time-varying delays," *Int. J. Robust Nonlinear Control*, vol. 30, no. 3, pp. 1035–1049, Feb. 2020.

[26] E. Y. Bejarbaneh, M. Masoumnezhad, D. J. Armaghani, and B. T. Pham, "Design of robust control based on linear matrix inequality and a novel hybrid PSO search technique for autonomous underwater vehicle," *Appl. Ocean Res.*, vol. 101, Aug. 2020, Art. no. 102231.

[27] Z. Zhuang, H. Tao, Y. Chen, V. Stojanovic, and W. Paszke, "An optimal iterative learning control approach for linear systems with nonuniform trial lengths under input constraints," *IEEE Trans. Syst., Man, Cybern., Syst.*, vol. 53, no. 6, pp. 3461–3473, Jun. 2023.

[28] C. K. Ahn, P. Shi, and M. V. Basin, "Two-dimensional dissipative control and filtering for Roesser model," *IEEE Trans. Autom. Control*, vol. 60, no. 7, pp. 1745–1759, Jul. 2015.

[29] L. Wang, H. Yang, and H. Tao, "Dynamic iterative learning control for linear repetitive processes over finite frequency ranges," *Control Decision*, vol. 36, pp. 599–608, Jan. 2021.

QINGFENG XIA received the B.S. degree in automation from Dalian Maritime University, in 2006, and the M.S. degree in pattern recognition and intelligent system from the University of Chinese Academy of Sciences, in 2009. He is currently pursuing the Ph.D. degree with Nanjing University, Nanjing, China. He is also an Associate Professor with Wuxi University, Wuxi, China. His research interests include intelligent control and multi-robot cooperation.

MENGHAN WEI received the bachelor's degree in automation (rail) from Binjiang College, Nanjing University of Information Engineering (NUIE), Wuxi. She is currently pursuing the master's degree in electronic information with the Graduate School, NUIE.

YIYANG CHEN (Member, IEEE) received the M.Eng. degree from Imperial College London, London, U.K., in 2013, and the Ph.D. degree from the University of Southampton, Southampton, U.K., in 2017. After that, he was a Research Fellow of control systems and a Research Fellow of traffic signal control with the University of Southampton, from 2017 to 2018 and from 2018 to 2020, respectively. He joined the School of Mechanical and Electrical Engineering, Soochow University, in 2020, as an Associate Professor. He has published several papers in top control conferences and journals. His research interests include iterative learning control, optimization, artificial intelligence, image processing, and robotic systems.

LEI WANG received the Ph.D. degree in control theory and control engineering from Jiangnan University, in 2021. He joined the Prince of Songkla University, Thailand, in 2013. He studied at Yunlin University of Science and Technology, Taiwan, in 2014. From 2018 to 2019, he studied at the University of Zielona Góra, Poland. His research interest includes iterative learning control.

LIANGXIN DONG received the bachelor's degree in material science and engineering from Harbin University of Technology. He is currently pursuing the master's degree in electronic information with Wuxi Graduate School, Nanjing University of Information Engineering. His scientific research achievements include two SCI journal published, two utility model patents have been authorized, and two invention patents have been submitted.